Kinetics of Membrane Raft Formation: Fatty Acid Domains in Stratum Corneum Lipid Models

David J. Moore,*,† Robert G. Snyder,‡ Mark E. Rerek,§ and Richard Mendelsohn||

International Specialty Products, 1361 Alps Road, Wayne, New Jersey 07470, College of Chemistry, University of California, Berkeley, California 94720, Reheis Corporation, 235 Snyder Ave., Berkeley Heights, New Jersey 07922, and Department of Chemistry, Newark College of Arts and Sciences, Rutgers University, 73 Warren Street, Newark, New Jersey, 07102

Received: August 29, 2005; In Final Form: November 22, 2005

The major barrier to permeability in skin resides in the outermost layer of the epidermis, the stratum corneum (SC). The major SC lipid components are ceramides, free fatty acids, and cholesterol. Ternary mixtures containing these constituents are widely used for physicochemical characterization of the barrier. Prior X-ray diffraction and IR spectroscopy studies have revealed the existence of ordered lipid chains packed in orthorhombic subcells. To monitor the kinetics of formation of regions rich in fatty acids, the current study utilizes a modification of the method (*J. Phys. Chem.* **1992**, *96*, 10008) developed to monitor component demixing in *n*-alkane mixtures. The approach is based on changes in the scissoring or rocking mode contours in the IR spectra of (orthorhombically packed) ordered chains. In the current study, equimolar mixtures of ceramides (either non-hydroxy fatty acid sphingosine ceramide or α-hydroxy fatty acid sphingosine ceramide) with chain perdeuterated fatty acids (either palmitic or stearic acid) and cholesterol reveal a time evolution of the scissoring contour of the deuterated fatty acid chains following quenching from relatively high temperatures where random mixing occurs. Segregation of domains enriched in the fatty acid component is observed. The kinetics of segregation are sensitive to the quenching temperature and to the chemical composition of the mixture. The kinetic regimes are conveniently catalogued with a power law of the form $P = Kt^{\alpha}$ where P is a (measured) property related to domain composition. The time scales for demixing in these experiments are similar to times observed in several studies that have tracked the restoration of the in vivo permeability barrier following nonthermal challenges to SC integrity. Further evidence for the physiological importance of the current measurements is the detection of these phases in native SC. The current work constitutes the first direct, structure-based determination of the kinetics of barrier formation in relevant skin lipid barrier models.

Introduction

The existence of lipid domains in model membrane systems including monolayers at the air/water interface and liposomes is well established.[1−3] Recent attention in this area has concentrated on "lipid rafts", i.e., plasma membrane domains enriched in sphingolipids and cholesterol.[4] The term raft, though not rigorously defined, generally designates a nonrandomly mixed cluster of ordered lipids containing closely packed acyl chains. The initial evidence for rafts, for example in plasma membranes, was based in part on the observation of detergent resistant membrane fractions enriched in the aforementioned components.[5] It has been quite reasonably proposed that the tight acyl chain packing of ordered membrane sphingolipids (which generally contain long saturated chains) is responsible for their detergent insolubility. The role of cholesterol is less well-defined, although it has been suggested that the sterol stabilizes the crystal−liquid interface in phospholipid monolayers.[6,7]

A plethora of biophysical methods have been used to attempt to estimate raft size and composition. The variation in results from such studies no doubt in part reflects the differing sensitivity, time scales, and length scales of the sampling technologies. A variety of biological functions have been proposed for ordered membrane lipid domains.[8−13] For example, such structures may be important for lipid and protein transport or for intracellular signaling.[8] In addition, a role for membrane domains in regulating integral membrane proteins has been suggested.

The stratum corneum (SC), the outer aspect of the epidermis, is known to contain lamellar membrane bilayers composed of sphingolipid-derived ceramides, fatty acids, and cholesterol. It is well documented that these lipids are highly ordered and packed in orthorhombic phases. Our previous IR studies of SC lipid models have demonstrated the presence of ordered lipid domains, a finding consistent with the domain mosaic model of SC lipid organization proposed by Forslind.[14−18] The function(s) of ordered lipid domains in the SC is likely driven by physical/structural requirements. The SC must be resilient, plastic, strong, flexible, and basically water impermeable; this combination of properties requires a complex heterogeneous material. However, it is also quite probable that lipid domains within the SC play a key role in regulating SC protein activity. This may be one of the mechanisms by which enzyme activity

* To whom correspondence should be addressed. E-mail: djmoore@ispcorp.com.
† International Specialty Products.
‡ University of California, Berkeley.
§ Reheis Corporation.
|| Rutgers University.

10.1021/jp054875h CCC: $33.50
Published on Web 01/17/2006

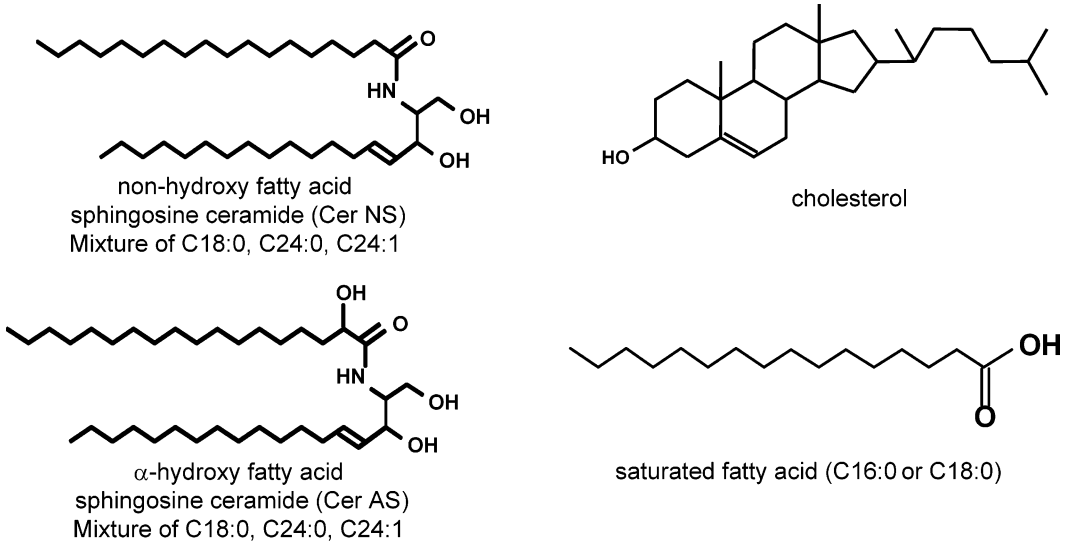

Figure 1. Chemical structures of the components of the SC model.

is regulated at different depths within the SC in order to control the desquamation process of the outer SC.

To further characterize SC domain formation, it is critical to understand the structure, phase behavior, and miscibility characteristics in binary and ternary mixtures composed of the major lipid classes in the skin barrier, i.e., ceramides, fatty acids, and cholesterol.[16,19−25] Domain size can be deduced from a variety of physical techniques, and molecular structure information (i.e., chain conformation and packing) about the domain constituents may be deduced from IR and Raman measurements. In view of the varying roles postulated for different lipid classes in the structure of SC, a determination of the kinetics of lipid domain formation (also termed clustering or "demixing" in the alkane hydrocarbon literature) is of significance for understanding the details of barrier structure. In addition, kinetic studies may have important physiological relevance. For example, as discussed below, dermal and transdermal delivery of drugs often requires (temporary) disruption of the SC lipid barrier.

However, molecular-based information about the kinetics of domain formation is lacking in lipid models for the SC and, of course, in the intact native SC. The current study addresses the first issue and utilizes a modified version of an IR spectroscopic method originally developed by Snyder and co-workers.[26−28] The method is discussed in the Material and Methods section below. In addition to its application to the study of demixing events in solid phases of *n*-alkanes, the general approach has been applied to monitor domain size and formation in saturated phosphatidylcholine mixtures and in esters.[29−31]

The studies reported here are divided into three parts. First, mixtures of proteated and deuterated C_{30} alkanes in the solid state are examined as a reference system to demonstrate the methods and to provide comparative characterizations for the scissoring contour in the SC models. Next, spectral parameters are acquired for the scissoring contours in isotopic mixtures of both stearic (FA_{18}^{H}/FA_{18}^{D}) and palmitic (FA_{16}^{H}/FA_{16}^{D}) acids. These two molecules serve as reference states (presumably ideal mixtures) for the fatty acid component of the ternary systems (ceramide/cholesterol/ fatty acid) used to model the SC. Finally, the reference state spectral parameters gained from these relatively simple model systems are applied to monitor the time evolution of domain formation in selected ceramide/fatty acid/ cholesterol mixtures. The chemical structures of the various constituents are given in Figure 1.

Materials and Methods

Materials and Sample Preparation. Cholesterol, non-hydroxy fatty acid sphingosine ceramide (CerNS), and α-hydroxy fatty acid sphingosine ceramide (CerAS) were purchased from Sigma Scientific. Perdeuterated palmitic acid (C16FA-d_{31}) and stearic acid (C18FA-d_{35}) were obtained from CDN Isotopes (Pointe Claire, Quebec, Canada). Equimolar samples of ceramide, cholesterol, and fatty acid were prepared by co-dissolving the lipids in chloroform/methanol, removing the solvent with N_2 and vacuum, after which the lipids were hydrated in excess citrate buffer (pH 5.5, approximate skin pH) by repeated cycles of heating to above Tm, cooling and mixing by vortex action.

Fourier Transform Infrared (FTIR) Spectroscopy. Maximally hydrated lipid samples (prepared as above) were sandwiched between AgCl IR windows and placed in a temperature-controlled transmission cell (Harrick Scientific, Ossining, NY). Experiments were initiated by heating samples to 90 °C and then cooling rapidly to the desired annealing temperature of 25, 30, or 35 °C. The cooling process took approximately 5 min. When the desired temperature was achieved, spectral acquisition commenced and continued for a period of at least 9 h with a spectrum being acquired every 15 min.

Spectra were acquired on a Mattson Infinity spectrometer equipped with a sample shuttle and a broad-band mercury−cadmium−telluride (MCT) detector. Spectra were generated from 256 co-added and ratioed interferograms collected at 2 cm^{-1} resolution. A macro was written in Mattson's WinFirst software (supplied with the spectrometer) that automated the process of spectral acquisition every 15 min. Spectra were analyzed off-line primarily using software written at the National Research Council of Canada and Grams (Thermo Galactic, Salem, NH). Plots were generated using SigmaPlot (SCSS, Chicago).

General IR Approach for Evaluation of Domain Formation. In the current study, the component concentrations of domains containing fatty acid and ceramide chains are determined using a variant of a method originally developed by Snyder and associates to study spontaneous demixing in crystalline binary *n*-alkane mixtures.[26−28] The method is based on observations that the shapes of the methylene scissoring and rocking bands in the IR spectra of a binary mixture of same-length hydrogenated and deuterated *n*-alkanes are highly de-

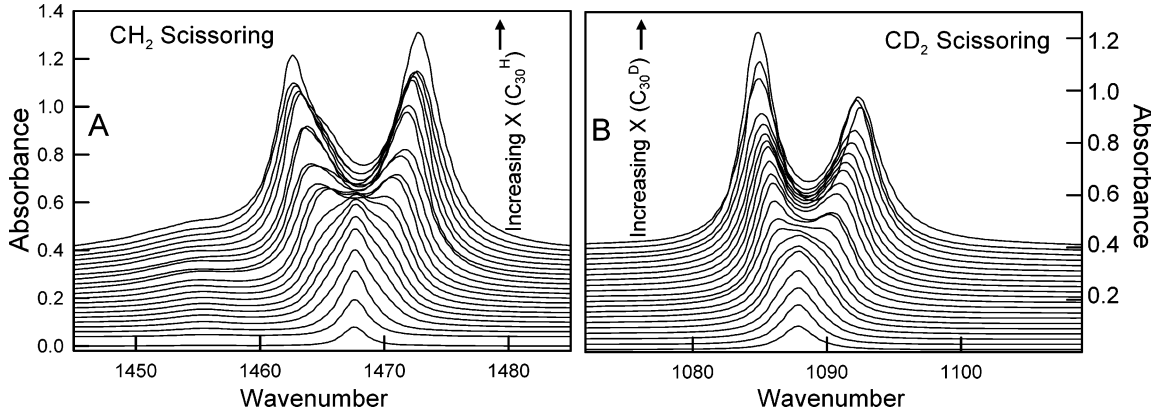

Figure 2. IR spectra of the methylene scissoring region for equilibrium solid-state binary mixtures of the straight chain alkanes, $C_{30}H_{62}$ and $C_{30}D_{62}$. (A) Spectra for the $C_{30}H_{62}$ component as its mole fraction is increased (bottom to top) from 0.025 to 1.0 in the following steps: 0.025, 0.054, 0.084, 0.152, 0.209, 0.252, 0.296, 0.348, 0.401, 0.461, 0.501, 0.549, 0.614, 0.646, 0.701, 0.739, 0.799, 0.848, 0.897, 0.941, 1.0. (B) Spectra of $C_{30}D_{62}$ component as its mole fraction is increased (bottom to top) from 0.059 to 1.0 in the following steps: 0.059, 0.103, 0.152, 0.201, 0.261, 0.299, 0.354, 0.386, 0.451, 0.499, 0.539, 0.599, 0.652, 0.704, 0.748, 0.791, 0.848, 0.906, 0.946, 0.975, 1.0.

pendent on component concentration and that this dependence is quantitatively independent of chain length for chains longer than about 20 carbons. It can be assumed that chain mixing in these solutions is random.

If the H and D *n*-alkanes in such mixtures differ in length, some degree of aggregation will occur and this is reflected in changes in shapes of the marker bands. Analyses of binary *n*-alkane mixtures (Department of Chemistry, UC Berkeley) indicates that chain mixing in the phases of partially demixed binary systems is also random. It then follows that the shapes of the bands observed in same-length binary mixtures can be used as a basis for analyzing chain aggregation, in systems where the chain lengths differ.

The dependence of the methylene scissors band shape on component concentration is illustrated in Figure 2 for *n*-$C_{30}H_{62}$/*n*-$C_{30}D_{62}$ mixtures. If the concentration of either component is low, less than 5%, the IR band associated with that component is a narrow singlet, whereas for the undiluted components it is a doublet consisting of narrow bands separated by ∼10.4 and 7.5 cm^{-1} for the proteated and deuterated components, respectively. In the middle concentration region, the band shows both the singlet and the doublet in broadened form. The doublet band separation is significantly reduced from its maximum value.

The near chain-length independence of the band shape dependency on concentration results from the lateral nature of the interchain vibrational coupling that is responsible for perturbing the frequencies of the scissoring and rocking vibrations. The chain−chain vibrational coupling is short range and occurs predominantly between nearest neighbors. The interactions extend over the full length of the chains. Consequently, end effects are relatively small. Finally, it is noted that the band-shape dependence on isotopic concentration results from negligible H−D chain coupling relative to the coupling between H−H and D−D chain pairs. This follows from the fact that the scissoring contour shape depends on interchain vibrational coupling.[28,29,32] H−D coupling is weak due to the large frequency difference between the CH_2 and CD_2 fundamental vibrations. Thus, if a single, ordered, proteated chain is isotopically diluted among deuterated chains (see Figure 2A), the scissoring vibration from this chain at ∼1467 cm^{-1} will remain a single band despite the other two criteria for splitting (conformationally ordered chains, orthorhombic perpendicular subcell) having been satisfied.[33,34]

Component concentrations of a given chain mixture were determined in the current work as follows: The fatty acid component in each mixture was deuterated. The reference mixtures consisted of a series of same length proteated and deuterated fatty acids, whose component isotopes corresponded to the mixture of interest. IR spectra were acquired over a range of compositions. Parameters characterizing the scissoring contour (halfwidth or peak separations) were used to calibrate the composition of the phase enriched in deuterated fatty acids. From these calibration curves, the time-dependent changes in the composition of the phases in the mixture of interest were determined.

Results

(1) C_{30}^{H}/C_{30}^{D} Solid Alkane Mixtures: Scissoring Modes. As noted above, the methylene scissoring spectral regions for each component of C_{30}^{H}/C_{30}^{D} solid *n*-alkane mixtures as a function of composition are depicted in parts A and B of Figure 2 for *n*-$C_{30}H_{62}$/*n*-$C_{30}D_{62}$ mixtures. In Figure 3A, the splitting between the components and the halfwidth of the scissoring contour of the C_{30}^{H} component in a series of binary mixtures with C_{30}^{D} are plotted as a function of composition. Similarly, in Figure 3B the splitting between the components and the halfwidth of the scissoring contour of the C_{30}^{D} component in a series of binary mixtures with C_{30}^{H} are plotted as a function of composition. In each instance, the increasing number of isotopically alike chains that interact as the mole fraction of that particular isotope is increased may be monitored using either parameter. The splitting can be directly monitored from mole fractions greater than ∼0.2 and 0.25 for the proteated and deuterated components, respectively. The frequency differences for the components of the split band reach a maximum of ∼10.4 cm^{-1} for C_{30}^{H} and ∼7.5 cm^{-1} for C_{30}^{D}. The halfwidth is a somewhat more useful parameter that can be monitored over the entire composition range and that displays a greater range in frequency than the splitting, reaching maximal values of ∼14 and 10 cm^{-1} for the proteated and deuterated components, respectively. Thus over the entire range of composition, the halfwidth parameter provides a measure of the composition of the particular component in the domain. In the current instance, since the C_{30} alkanes are assumed to be ideally mixed, the measured halfwidths can be used to estimate the extent of demixing.

Although the above procedures may, in principle, be experimentally accomplished for any particular molecule of interest, the characterization of the scissoring contour as undertaken in

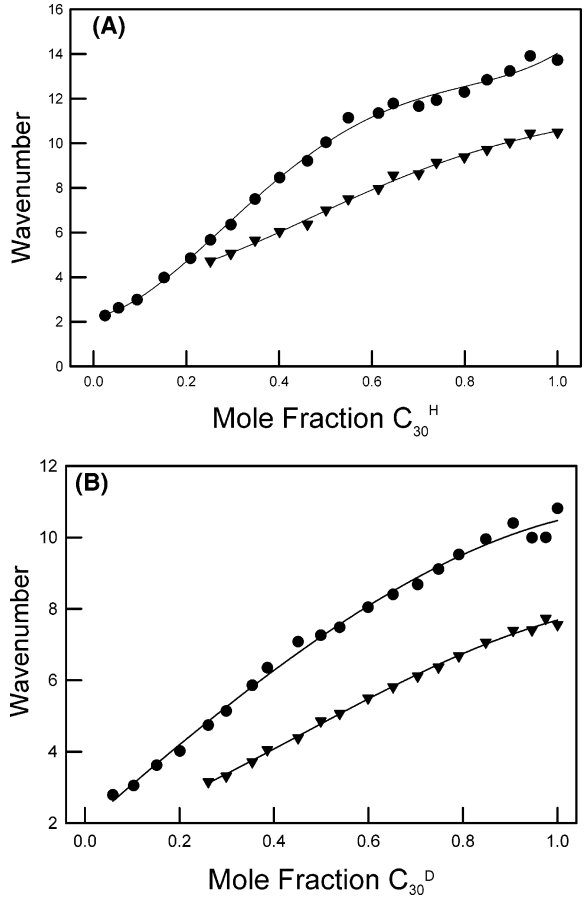

Figure 3. (A) Characterization of the scissoring splitting contour for $C_{30}H_{62}$ in binary mixtures with $C_{30}D_{62}$ using the half-width of the scissoring contour (●) or the splitting between the components of the contour (▼) as a function of mole fraction. (B) Characterization of the scissoring splitting contour for $C_{30}D_{62}$ in binary mixtures with $C_{30}H_{62}$ using the half-width of the scissoring contour (●) or the splitting between the components of the contour (▼) as a function of mole fraction.

Figure 3 for long-chain *n*-alkanes cannot be applied to estimate domain compositions in the ceramide component of the ternary SC model for three reasons. First, both CerNS and AS are naturally derived and contain a mixture of chain lengths (C18, C24, C24:1), whose scissoring splitting is not the same as in *n*-alkanes. Second, completely deuterated analogues of these molecules, which would be required for the construction of appropriate calibration curves in ternary models, are not currently available. Finally, CerNS and AS each have two covalent chains in the structure. This provides additional broadening of the contour each at low mole fractions of proteated constituent in the mixture. Thus it was decided for these initial kinetic studies of model SC systems, to treat only the fatty acid constituents (stearic acid-d_{35} or palmitic acid-d_{31}) quantitatively.

(2) Mixtures of Deuterated and Proteated Stearic Acid (FA_{18}^{H}/FA_{18}^{D}) and Palmitic Acid (FA_{16}^{H}/FA_{16}^{D}): Scissoring Modes. The fatty acid components of the SC differ from the alkane models both in chain length and by the possession of polar headgroups, each of which may significantly influence fatty acid chain-packing characteristics. In addition, the first few methylenes adjacent to the polar headgroup are perturbed in frequency compared with the alkanes, thereby affecting the vibrational coupling. Evidence for these effects[35,36] comes from observations that the maximal scissoring band splitting in a series of diacylphospholipids was chain length dependent. Thus

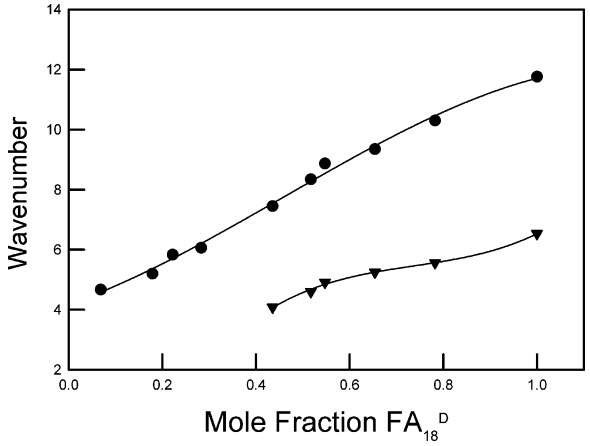

Figure 4. Characterization of the scissoring splitting contour for perdeuterated stearic acid (FA_{18}) in binary mixtures with its proteated isomer using the half-width of the scissoring contour (●) or the splitting between the components of the contour (▼) as a function of mole fraction.

separate calibration curves were required for these components. Since both stearic and palmitic acids have been used in models of the SC lipid barrier, composition vs bandwidth (or splitting) calibration curves were obtained for mixtures of the deuterated and proteated forms of each of these species. The data for the deuterated components are shown below since these are required for the model SC systems.

The frequencies and band splitting of the scissoring contour of the FA_{18}^{D} component in mixtures with FA_{18}^{H} are plotted as a function of composition in Figure 4. Below mole fractions of ~0.4, only a single peak is noted arising, as discussed above, from isolated or nearly isolated chains. As the mole fraction increases, the splitting increases to a maximum of ~6.5 cm^{-1}, which is, as anticipated, significantly lower than that for the deuterated C_{30} alkane. The bandwidth of the scissoring contour for the FA_{18}^{D} is also plotted in Figure 4 and, as for the alkanes, encompasses a greater range of mole fraction and frequency. The data in each curve are fit to a fourth-order polynomial to facilitate interpolation between data points, as required for the kinetic studies.

Kinetics of Domain Formation in Model Systems for the SC

The kinetics of domain formation was studied in four three-component equimolar systems, namely, CerNS/cholesterol/stearic acid-d_{35}, CerAS/cholesterol/stearic acid-d_{35}, CerNS/cholesterol/palmitic acid-d_{31}, and CerAS/cholesterol/palmitic acid-d_{31}. Each sample was initially heated to 90 °C and then quenched in separate experiments to setting temperatures of 25, 30, and 35 °C. The kinetics of domain formation of the fatty acid component were monitored for at least 9 h through the time evolution of the line widths and the onset of splitting of the methylene scissoring contours. Typical behavior of the time evolution of the scissoring contours of the fatty acid components is shown in parts A and B of Figure 5 for CerNS/cholesterol/stearic acid-d_{35}, (equimolar) and for CerAS/cholesterol/stearic acid-d_{35} (equimolar), respectively, at quenching temperatures of 35 °C. Equivalent data were collected for CerNS/cholesterol/palmitic acid-d_{31} and CerAS/cholesterol/palmitic acid-d_{31} (not shown), and all four lipid mixtures were quenched to 25 and 30 °C in addition to the 35 °C quenching experiments.

The time evolution of the perdeuterated fatty acid domains as monitored from the scissoring contour broadening are shown

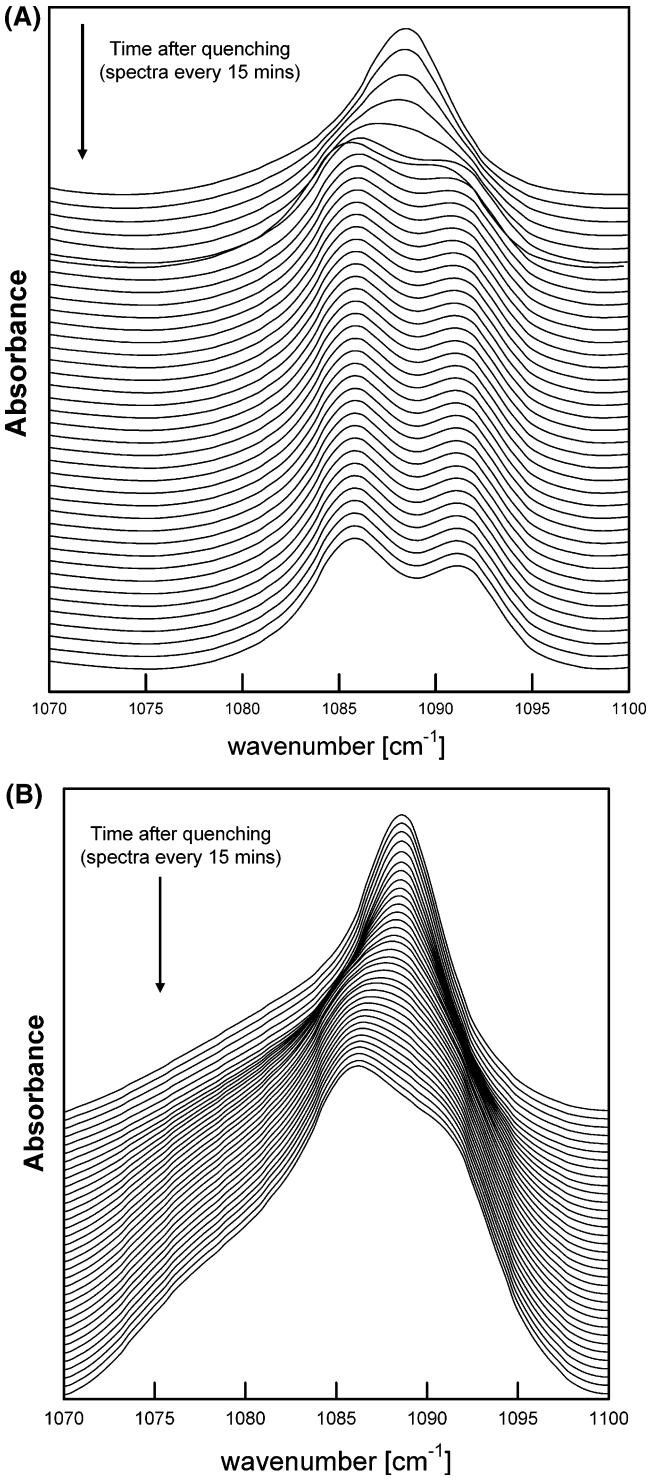

Figure 5. (A) Time evolution of the scissoring contour of the fatty acid component in the ternary model SC system CerNS/cholesterol/stearic acid-d_{35} (equimolar). (B) Time evolution of the scissoring contour of the fatty acid component in the ternary model SC system CerAS/cholesterol/stearic acid-d_{35} (equimolar). In each case, the setting temperature was 35 °C. Data were collected at 15 min. intervals for ~9 h.

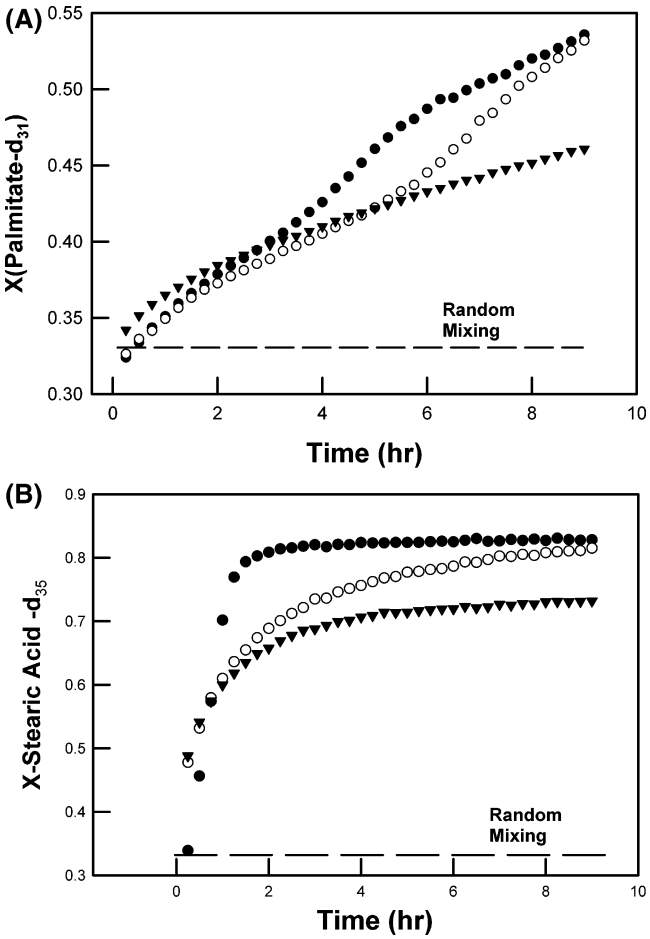

Figure 6. (A) The time evolution of palmitic acid-d_{31} domains in the equimolar ternary mixture CerNS/cholesterol/palmitic acid-d_{31}. The domain composition is represented as the mole fraction of palmitic acid chains in the domain as deduced from the halfwidth of the CD_2 scissoring contour. Data are shown for three different setting temperatures as follows: 35 °C (●); 30 °C (○); 25 °C (▼). (B) The time evolution of stearic acid-d_{35} domains in the equimolar ternary mixture CerNS/cholesterol/stearic acid-d_{35}. The domain size is represented as the mole fraction of stearic acid-d_{35} chains in the domain as deduced from the halfwidth of the CD_2 scissoring contour. Data are shown for three different setting temperatures as follows: 35 °C (●); 30 °C (○); 25 °C (▼).

in parts A and B of Figure 6 for CerNS/cholesterol/palmitic acid-d_{31} and CerNS/cholesterol/stearic acid-d_{35}, respectively, at 25, 30, and 35 °C. The CD_2 scissoring region spectra of the CerAS containing samples showed a broad composition-dependent spectral feature near 1076 cm^{-1} (see Figure 5B and compare with Figure 5A), which precluded measurements of the half-width of this contour. Included in parts A and B of Figure 6 are horizontal lines indicative of random mixing (mole fraction = 0.33). It is noted that the CerNS/cholesterol/palmitic acid-d_{31} remained in a randomly mixed state during quenching to 25, 30, or 35 °C while the CerNS/cholesterol/stearic acid-d_{35} system was only randomly mixed, under the conditions of these experiments, when the system was quenched to a temperature of 35 °C.

Interesting variations in the time evolution of domains between samples and between temperatures for a given sample are evident in the data. The composition of stearic acid-d_{35} reached a limiting value ($X = \sim 0.8$) which was significantly higher than that approached by palmitic acid ($X = \sim 0.55$) at the end of a 9-h period. In all cases the time for domain formation was more rapid at 35 °C than at lower temperatures, while segregation of stearic acid-d_{35} enriched domains is much more rapid for a given ceramide than palmitic acid-d_{31}-enriched domains.

The composition of domains formed in the (proteated) ceramide constituent cannot be measured quantitatively (heterogeneous chain length, no deuterated reference materials). In addition, the scissoring mode spectral region is overlapped from

cholesterol vibrations. Although the rocking modes near 720 cm^{-1} also split as a result of interactions between chains, the splitting or line width changes cannot be converted to domain compositions.

Discussion

Three aspects of the current results are presented. First, the biological relevance of these measurements for the recovery of the skin barrier following challenges to its integrity is considered. Second, the advantages and limitations of the current approach for evaluation of domain composition are elaborated. Finally, these initial results for the SC lipid models are evaluated within the framework of a model evaluated by Snyder and colleagues for the kinetics of *n*-alkane demixing.[34]

Biological Relevance

The current findings are considered in relation to the in vivo skin lipid barrier and the impact of physical and chemical stresses upon lipid dynamics and hence skin barrier function. As a practical example of the importance of understanding the kinetics of barrier reformation, we note that the dermal and transdermal delivery of drugs often requires disruption of the SC lipid barrier, whether by physical or chemical means. In general, direct physical characterization of barrier reformation kinetics has not been available. Prior studies, typified by those cited below, have used indirect physical characterizations of barrier function following perturbative treatments.

To evaluate the relevance of the time scales measured in the current experiments to those of the native barrier, we refer to several prior studies that used for the most part, nonstructurally oriented measurements. These studies, which employed a range of barrier disrupting stresses, including solvent treatment, UV−B radiation, and iontophoresis all report barrier recovery times from 24 to 144 h for complete recovery.[37−40] The only structurally oriented kinetics measurement of barrier reformation that we have found tracked the restoration of chain conformational order following oleic acid induced perturbations and reported 5.5 h for a 50% recovery of the frequency shift and 24 h for a full recovery, comparable with the current study of a three component skin barrier model.[41]

The above studies report on kinetic events occurring with time scales from 0.5 h to days. These durations are in qualitative accord with the direct measurements of orthorhombic domain formation following thermal perturbation in the SC models observed here and point to the relevance of the current experiments for biological processes in intact skin. From a practical point of view, the current study indicates that depending on the temperature and molecular organization of the SC lipid barrier, a "window" of several hours may be available before barrier lipid organization, and hence barrier function is restored following its disruption. It also clearly suggests that barrier temperature will dramatically impact the kinetics of lipid reorganization.

Advantages and Limitations of the Current Approach

The current method for characterization of fatty acid domains requires the explicit assumption made here that the fatty acid mixtures $C_{18}{}^{D}/C_{18}{}^{H}$ and $C_{16}{}^{D}/C_{16}{}^{H}$ mix ideally and thus provide the spectral characterization (line widths, splitting) defining particular domain compositions. We have been unable to find any studies on the occurrence of nonideality in fatty acid isotopic mixtures. Buckingham and Hentschel[42] have studied alkane mixtures theoretically and predicted that isotope segregation

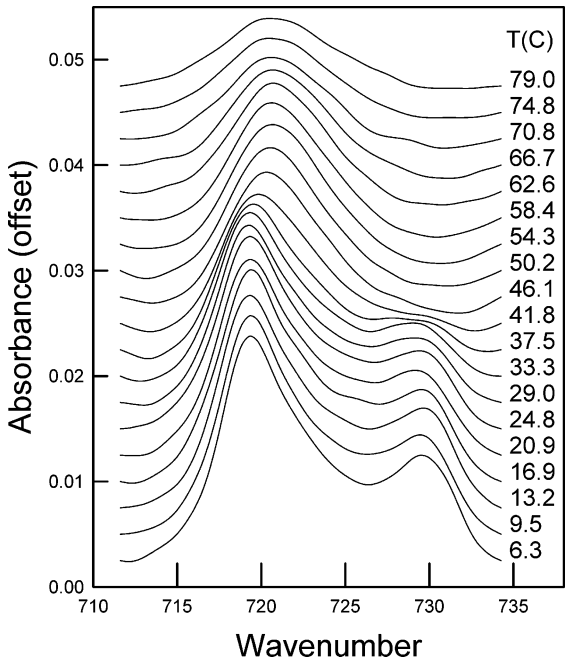

Figure 7. Temperature evolution of the rocking mode contour for native human SC.

phenomena are impossible for "small" hydrocarbons. It has been suggested[34] that, for the $C_{36}{}^{H}/C_{36}{}^{D}$ pair of alkanes, deviations from ideal mixing appear small and would be expected to be smaller still for the significantly shorter chains used here. Thus, with regard to the chain lengths used here, the assumption of ideal mixing for the isotopic species is justified. The presence of a polar headgroup permits additional specific interactions between polar moieties, which as a first approximation should not be dependent on chain deuteration.

Two additional structural criteria must be obeyed for the methylene scissoring method to be applicable to the study of domain formation. The first is that the lipid subcells formed in the domains be orthorhombic perpendicular. For these SC models, such phases have been detected both by X-ray diffraction and by IR spectroscopy. In addition, the relevance of the models to the native tissue has been demonstrated by prior IR studies in both intact SC[43] and in isolated SC lipids.[44] The existence of these phases in isolated SC is demonstrated in Figure 7 for the CH_2 rocking region. This spectral region responds to domain formation in similar fashion as the scissoring region. The temperature evolution of the rocking contour in intact (human) SC is also shown in Figure 7. These data clearly reveal an orthorhombic−hexagonal transition near ∼40 °C as measured by collapse of the initial doublet. All these observations provide strong evidence for the relevance of the current experiments to the formation and structure of the native barrier.

The validity of the concentration measurement in fatty acid enriched domains depends on the transferability of the parameters that characterize the scissoring contour from the calibration system (fatty acid isotopic mixtures) to the SC model. The potentially confounding issue is that in the ideally mixed systems used to calibrate the spectral response, the isotopic splitting is reduced by interaction of the deuterated chains with proteated chains of the same length and headgroup, whereas in the SC model, the splitting is reduced upon interaction of the deuterated fatty acid with the structurally very different cholesterol or ceramide components. The advantages of choosing the current spectral parameter (half width of the scissoring contour) to characterize the domains is that the line width increase upon

fatty acid segregation depends primarily on increased interaction between deuterated chains. Therefore changes in the central component of a contour that might result from slight differences in a deuterated chain frequency when it interacts with a ceramide or cholesterol compared to changes that occur upon interaction with a (proteated) fatty acid, are not likely to substantially affect the width of the contour.

Generic Framework for the Observed Time Evolution of Domains

To provide a theoretical framework for this kinetic experiment, we follow the Berkeley group[34] who evaluated the time dependence of demixing in alkanes from log−log plots of the domain size vs time following quenching, following some theoretical and experimental work based on diffusion processes suggesting a power law relation of the form $P = Kt^{\alpha}$ where P is a property related to domain size and K is a constant.

Log−log plots of the fatty acid domain composition versus time for the CerNS/cholesterol/palmitic acid and CerNS/cholesterol/stearic acid mixtures at the three setting temperatures are shown in parts A and B of Figure 8, respectively. These plots are nonlinear, and the data for CerNS/cholesterol/palmitic acid at 35 °C depict a sigmoidal function. Similarly shaped plots have been observed for *n*-alkanes.[34] The generic sigmoidal behavior depicted in Figure 9, which includes two "breaks" termed π and σ, was proposed to encompass a range of behaviors for the time evolution of domains.

For the CerNS/cholesterol/palmitic acid mixtures shortly after quenching, all three mixtures exhibit a palmitic acid domain composition close to that of random mixing, which is depicted as a horizontal line in Figure 8A. Different time regimes within the sigmoidal function appear to have been sampled during domain formation at the three setting temperatures utilized. Regions of the generic curve sampled at each quench temperature are schematically depicted in Figure 9. Thus, only the early region of the generic curve was sampled in the kinetic behavior of the mixture quenched at 25 °C (slowest rate of domain formation), the π break was sampled in the mixture quenched at 30 °C, and both the π and σ breaks were observed for the most rapid domain formation in the mixture quenched at 35 °C. The above analysis cannot be applied to the CerNS/cholesterol/stearic acid mixture. In this instance, only the sample set to 35 °C exhibits a fatty acid domain composition close to that of random mixing. We speculate that the CerNS/cholesterol/stearic acid system (35 °C quenching temperature) encompasses only the σ transition, suggesting relatively rapid early kinetics.

Possible structural origins of the π and σ breaks have been previously discussed.[34] The π break may reflect a structural modification in which increased conformational ordering occurs in the interlayer region. This break is most likely to be visible for the longest chain component of the mixture. In the current case, when the longer ceramide chains are diluted by the presence of cholesterol or fatty acid, the ends of these chains are likely to be conformationally disordered. As domain formation begins, the ordering of the (ceramide) chains increases resulting in the appearance of some void space, which it is suggested, might tend to increase the overall rate of diffusion leading to domain formation.

Evidence for the above description could come from examination of the time evolution of CH_2 stretching frequencies. Prior to utilizing these modes to directly monitor conformational order, some background considerations are required. Whereas the methylene scissoring vibrations are very sensitive to domain size and intermolecular packing, the methylene stretching

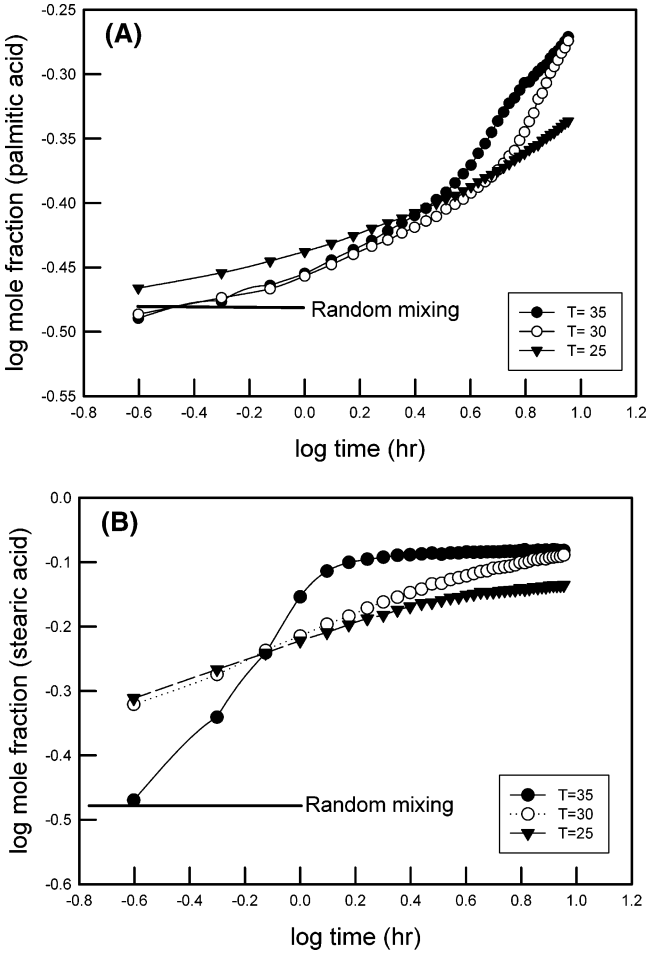

Figure 8. (A) log−log plot of the time evolution of palmitic acid-d_{31} domains in the equimolar ternary mixture CerNS/cholesterol/palmitic acid-d_{31}. The domain size is represented as the mole fraction of palmitic acid chains in the domain as deduced from the halfwidth of the CD_2 scissoring contour. Data are shown for three different setting temperatures as follows: 35 °C (●); 30 °C (○); 25°C (▼). The scissoring splitting expected for random mixing is depicted as a horizontal line at an ordinate position of −0.477 (log 1/3). Note that shortly after quenching, all three mixtures exhibit a fatty acid domain composition close to that of random mixing, which is depicted as a horizontal line. (B) log−log plot of the time evolution of stearic acid-d_{31} domains in the equimolar ternary mixture CerNS/cholesterol/stearic acid-d_{35}. The domain size is represented as the mole fraction of palmitic acid chains in the domain as deduced from the halfwidth of the CD_2 scissoring contour. Data are shown for three different setting temperatures as follows: 35 °C (●); 30 °C (○); 25 °C (▼). Note that shortly after quenching, only the mixture quenched at 35 °C exhibits a fatty acid domain composition close to that of random mixing, which is depicted as a horizontal line.

vibrations are sensitive to intrachain conformational order/disorder processes. The introduction of conformational disorder into the chains increases both the symmetric and asymmetric CH_2 stretching frequency (∼2850 and 2920 cm^{-1}, respectively) by several cm^{-1}. If the methylene stretching mode frequencies were sensitive only to conformational order, it would be anticipated that plots of these frequencies as a function of composition in solid fatty acid mixtures would be horizontal since the fatty acid mixtures are in fully ordered crystalline phases at the temperatures studied. However, the experimental results (Figure 10) reveal an additional effect.

The composition dependence of $FA_{18}{}^{H}$ and $FA_{18}{}^{D}$ on the CH_2 and CD_2 asymmetric stretching modes stretching modes are plotted in parts A and B of Figure 10, which shows that the asymmetric CH_2 symmetric stretching mode of $FA_{18}{}^{H}$ decreases

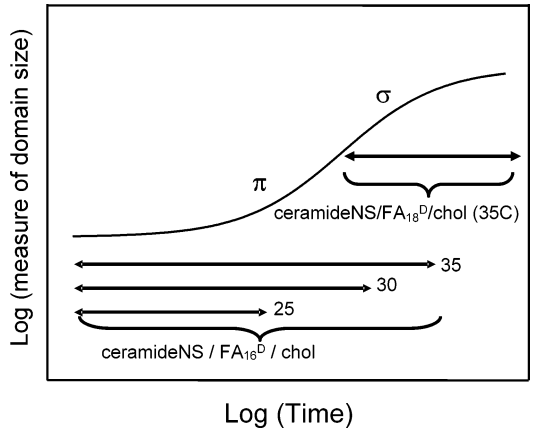

Figure 9. Generic model for the kinetics of domain formation depicted as a sigmoid log−log plot. The CerNS/cholesterol/palmitic acid-d_{31} system, quenched at 25, 30, or 35 °C, samples part or the entire curve as indicated schematically on the plot. The CerNS/cholesterol/palmitic acid-d_{35} system quenched at 35 °C samples the σ transition region of the curve. See text for discussion.

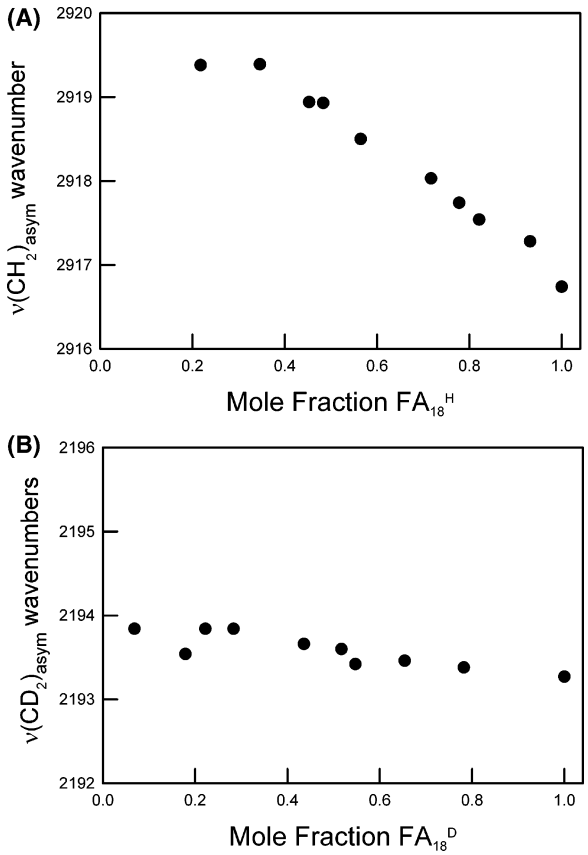

Figure 10. Composition dependence of (A) the CH_2 asymmetric stretching frequency of stearic acid-h_{35} in binary mixtures with stearic acid-d_{35} (B) the CD_2 asymmetric stretching frequency of stearic acid-d_{35} in binary mixtures with stearic acid-h_{35}.

by ∼2.8 cm^{-1}, respectively, as its mole fraction increases from 0.2 to 1. Since the chains are fully ordered at all mole fractions, this decrease must reflect interchain interactions. This decrease is quite significant, as the entire range of variation for the frequency of this mode is typically ∼9 cm^{-1} for (2916−2125 cm^{-1}). Thus ∼30% of the variation may come from lateral interactions in ordered phases. Similar results have been documented by Lafleur and co-workers.[45] The composition dependence of the CD_2 asymmetric stretching frequency of FA_{18}^D plotted in Figure 10 shows that frequency to be much

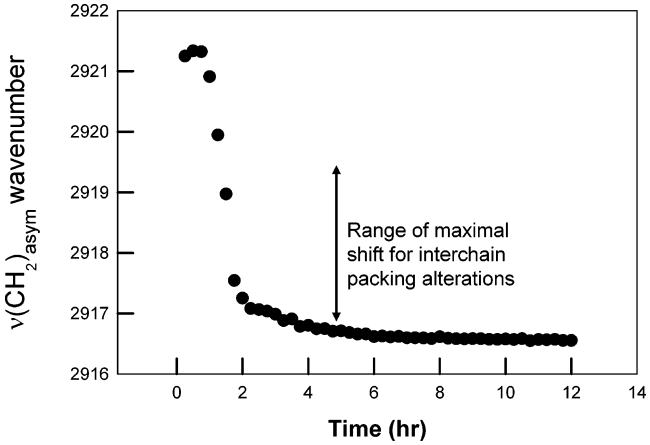

Figure 11. Time evolution of conformational ordering of CerNS in ternary mixture with cholesterol and palmitic acid-d_{31}, quenched at 35 °C as sampled from the methylene asymmetric CH_2 stretching frequency. An initial lag period, followed by substantial conformational ordering, is evident.

less sensitive to lateral interactions than its proteated counterpart. There is a relatively small frequency decrease of ∼0.5 cm^{-1} as the mole fraction increases from 0.05 to 1 compared with the proteated mode, which decreases by ∼2.8 cm^{-1}.

In Figure 11is shown the time evolution of CH_2 stretching frequencies of the ceramide component plotted for CerNS/cholesterol/stearic acid-d_{35} mixtures. The CH_2 asymmetric stretching frequency decreases significantly with time after an initial lag period, consistent with conformational ordering increasing as the phase separation events take place. It is noted that the range of change of the frequency (∼4.8 cm^{-1}) is significantly greater than the maximal range of change (∼2.8 cm^{-1}) arising from interchain interactions (see Figure 10A). Thus we conclude that at least ∼40% (2/4.8) of the frequency decrease in Figure 11 arises from conformational ordering in the chain.

The σ break delineates a slowing of the growth rate since the availability of the particular "mixed" component becomes limited. Small, unstable domains become depleted and incorporated into larger ones.

In conclusion, the current experiments suggest that the method developed by Snyder and associates mostly for the kinetics of demixing in binary alkane mixtures may be profitably extended to standard three component models of the SC barrier and possibly to the native SC. The time scales for segregation of the fatty acid rich domains are generally similar to the time scales observed for restoration of the skin barrier in both native skin and purified SC using analytical methods that are not structurally oriented. Thus, the current results may eventually provide a direct structural/kinetic model for the formation of the barrier that will be an important addition/extension over functional evaluations (TEWL, barrier resistance) currently used.

Acknowledgment. This work was supported by PHS grant GM 29864 to R.M. Dina Van Wyck is thanked for her excellent technical assistance.

References and Notes

(1) McConnell, H. M. *Annu. Rev. Phys. Chem.* **1991**, *42*, 171.
(2) Mohwald, H. *Annu. Rev. Phys. Chem.* **1990**, *41*, 441.
(3) Edidin, M. *Annu. Rev. Biophys. Biomol. Struct.* **2003**, *32*, 257.
(4) Brown, D. A.; London, E. *J. Membr. Biol.* **1998**, *164*, 103.
(5) London, E.; Brown, D. A. *Biochim. Biophys. Acta* **2000**, *1508*, 182.
(6) McConnell, H. M.; Radhakrishnan, A. *Biochim. Biophys. Acta* **2003**, *1610*, 159.

(7) Silvius, J. R. *Biochim. Biophys. Acta* **2003**, *1610*, 174.
(8) Simons, K.; Ikonen, E. *Nature* **1997**, *387*, 569.
(9) Brown, D. A.; London, E. *Annu. Rev. Cell Dev. Biol.* **1998**, *14*, 111.
(10) Helms, J. B.; Zurzolo, C. *Traffic* **2004**, *5*, 247.
(11) Salaun, C.; James, D. J.; Chamberlain, L. H. *Traffic* **2004**, *5*, 255.
(12) Devaux, P. F.; Morris, R. *Traffic* **2004**, *5*, 241.
(13) Mayor, S.; Rao, M. *Traffic* **2004**, *5*, 231.
(14) Moore, D. J.; Rerek, M. E.; Mendelsohn, R. *Biochem. Biophys. Res. Commun.* **1997**, *231*, 797.
(15) Moore, D. J.; Rerek, M. E. *Acta Derm. Venereol.* **2000**, *Supp 208*, 16.
(16) Mendelsohn, R.; Moore, D. J. *Methods In Enzymology: Sphingolipid Metabolsim and Cell Signaling*; Hannun, Y. A., Merrill, A. H., Eds.; Academic Press: 2000; p 312,
(17) Rerek, M. E.; Wyck, D. V.; Mendelsohn, R.; Moore, D. J. *Chem. Phys. Lipids* **2005**, *134*, 51.
(18) Forslind, B. *Acta Derm. Venereol.* **1994**, *74*, 1.
(19) Kitson, N.; Thewalt, J.; Lafleur, M.; Bloom, M. *Biochemistry* **1994**, *33*, 6707.
(20) Bouwstra, J. A.; Thewalt, J.; Gooris, G. S.; Kitson, N. *Biochemistry* **1997**, *36*, 7717.
(21) Lafleur, M. *Can. J. Chem.* **1998**, *76*, 1501.
(22) Thewalt, J.; Kitson, N.; Araujo, C.; MacKay, A.; Bloom, M. *Biochem. Biophys. Res. Commun.* **1992**, *188*, 1247.
(23) Grotenhuis, E. T.; Demel, R. A.; Ponec, M.; Boer, D. R.; Miltenburg, J. C. v.; Bouwstra, J. A. *Biophys. J.* **1996**, *71*, 1389.
(24) Pilgram, G. S. K.; Engelsma-van Pelt, A. M.; Oostergetel, G. T.; Koerten, H. K.; Bouwstra, J. A. *J. Lipid Res.* **1998**, *39*, 1669.
(25) Abraham, W.; Downing, D. T. *Pharm. Res.* **1992**, *9*, 1415.
(26) Snyder, R. G. *J. Mol. Spectrosc.* **1960**, *4*, 411.
(27) Snyder, R. G. *J. Mol. Spectrosc.* **1961**, *7*, 116.
(28) Snyder, R. G. *J. Chem. Phys.* **1979**, *71*, 3229.
(29) Snyder, R. G.; Strauss, H. L.; Cates, D. A. *J. Phys. Chem.* **1995**, *99*, 8432.
(30) Mendelsohn, R.; Liang, G. L.; Strauss, H. L.; Snyder, R. G. *Biophys. J.* **1995**, *69*, 1987.
(31) Snyder, R. G.; Liang, G. L.; Strauss, H. L.; Mendelsohn, R. *Biophys. J.* **1996**, *71*, 3186.
(32) Snyder, R. G.; Conti, G.; Strauss, H. L.; Dorset, D. L. *J. Phys. Chem.* **1993**, *97*, 7342.
(33) Mendelsohn, R.; Moore, D. J. *Chem. Phys. Lipids* **1998**, *96*, 141.
(34) Snyder, R. G.; Goh, M. C.; Srivatsavoy, V. J. P.; Strauss, H. L.; Dorset, D. L. *J. Phys. Chem.* **1992**, *96*, 10008.
(35) Cameron, D. G.; Casal, H. L.; Gudgin, E. F.; Mantsch, H. H. *Biochemistry* **1980**, *19*, 3665.
(36) Yan, W.-Y.; Strauss, H. L.; Snyder, R. G. *J. Phys. Chem. B* **2000**, *104*, 4229.
(37) Grubauer, G.; Elias, P. M.; Feingold, K. R. *J. Lipid Res.* **1989**, *30*, 323.
(38) Hatziantoniou, S.; Rallis, M.; Demetzos, C.; Papaioannou, G. T. *Pharmacol. Res.* **2000**, *42*, 55.
(39) Craane-Van Hinsberg, I. W. H. M.; Verhoef, J. C.; Spies, F.; Bouwstra, J. A.; Gooris, G. S.; Junginger, H. E.; Bodde, H. E. *Microsc. Res. Tech.* **1997**, *37*, 200.
(40) Curdy, C.; Kalia, Y. N.; Falson-Rieg, F.; Guy, R. H. *AAPS PharmSci* **2000**, *2*, 1.
(41) Mak, V. H. W.; Potts, R. O.; Guy, R. H. *J. Controlled Release* **1990**, *12*, 67.
(42) Buckingham, A. D.; Hentshel, H. G. E. *J. Polym. Sci., Phys. Ed.* **1980**, *18*, 853.
(43) Bouwstra, J. A.; de Graaff, A.; Gooris, G. S.; Nijsse, J.; Wiechers, J. W.; van Aelst, A. C. *J. Invest. Dermatol.* **2003**, *120*, 750.
(44) Ongpipattanakul, B.; Francoeur, M. L.; Potts, R. O. *Biochim. Biophys. Acta* **1994**, *1190*, 115.
(45) Kodati, V. R.; El-Jastmi, R.; Lafleur, M. *J. Phys. Chem.* **1994**, *98*, 12191.